String model building using Quantum Annealers

Ioannis Rizos

Physics Department, University of Ioannina

BWXX SEENET-MTP Meeting
August 29 – 31, 2023 Vrnjačka Banja, Serbia

String Theory

String theory is our best candidate for the consistent description of all interactions including gravity.

String theory is formulated in 10 spacetime dimensions where we have five consistent theories: Type IIA and IIB, $E_8 \times E_8$ and $SO(32)$ heterotic (closed strings), and Type I theory (open strings). These string theories are related by symmetries (dualities) and are believed to come from a fundamental 11-dimensional theory called M-theory.

String Phenomenology

To make contact with particle physics phenomenology we have to "compactify" string theory down to four spacetime dimensions. This leads to a huge number of "vacua" in four dimensions. Rough estimates give 10^{500} or even much higher.

String phenomenology aims at studying string vacua with properties close to the Standard Model or some of its extensions. This entails extensive scans over the vast parameter space of the string compactifications. To this end, several methods have been employed including direct comprehensive search of parts of the parameter space, genetic algorithms, methods based on machine learning.

In a recent work we have considered the use of quantum adiabatic algorithms and more specifically an approach known as Quantum Annealing (QA) in the search of phenomenologically promising string vacua.

S. Abel, L. A. Nutricati, I. R., *arXiv:2306.16801*

Quantum Annealers

Simulated annealing is an algorithm that can find global solutions to optimization problems. It is often used for functions of discrete variables with numerous optima. From the physics point of view, a system representing the problem is considered at finite temperature. The ground state of the system corresponds to a solution of the problem. To approach the solution, we initially put the system in relatively high temperature and find its equilibrium state. We then lower the temperature slowly, as to maintain equilibrium, and eventually reach the ground state at zero temperature.

Quantum annealers follow a similar procedure, but they use quantum fluctuations instead of thermal fluctuations. The problem is translated into an interacting Ising-spin model and quantum fluctuations are induced by the transverse field.

Several studies have shown that quantum annealing outperforms simulated annealing.

Implementation of Quantum Annealing

D-Wave offers a fully functional quantum annealing implementation. The Hamiltonian can be recast in the form

$$H_{\text{sing}} = -\frac{A(t)}{2} \underbrace{\left(\sum_i \sigma_x^{(i)} \right)}_{\text{Initial Hamiltonian}} + \frac{B(t)}{2} \underbrace{\left(\sum_i h_i \sigma_z^{(i)} + \sum_{i>j} J_{i,j} \sigma_z^{(i)} \sigma_z^{(j)} \right)}_{\text{Problem Hamiltonian}}$$

where $\sigma_x^{(i)}$, $\sigma_z^{(i)}$ are Pauli matrices ascribed to the qubit q_i, h_i are the qubit biases and $J_{i,j}$ are the coupling strengths. The functions $A(t), B(t)$ are adjusted by the system: Normally, annealing begins at $t = 0$ with $A(t) \gg B(t)$ and ends at $t = 1$ with $A(t) \ll B(t)$.

Impementation of Quantum Annealing

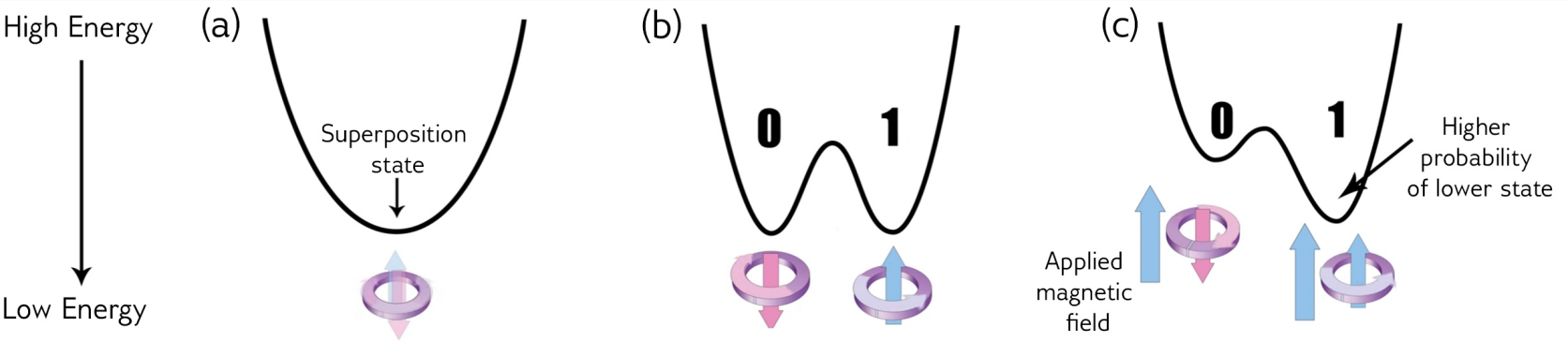

Figure 1: Energy diagram changes over time as the quantum annealing process runs and a bias is applied.

In summary, the systems starts with a set of qubits, each in a superposition state of 0 and 1. They are not yet coupled. When they undergo quantum annealing, the couplers and biases are introduced and the qubits become entangled. At this point, the system is in an entangled state of many possible answers. By the end of the anneal, each qubit is in a classical state that represents the minimum energy state of the problem, or one very close to it. All of this happens in D-Wave quantum computers in a matter of microseconds.

A simple example

To solve the equation

$$2x + 3y = 5, (x, y) \in \{-1, 1\}$$

on a quantum annealer, we minimize

$$(2x + 3y - 5)^2 = 4x^2 + 12xy - 20x + 9y^2 - 30y + 25$$

Thus we utilize the Ising model (problem Hamiltonian)

$$H = \sum_i h_i \sigma_z^{(i)} + \sum_{i>j} J_{i,j} \sigma_z^{(i)} \sigma_z^{(j)}$$

with

$$h_1 = -20, h_2 = -30 \ , \ J_{i,j} = \begin{pmatrix} 4 & 12 \\ 0 & 9 \end{pmatrix} .$$

Solving a slightly different version of the same equation

$$2x + 3y = 5 \mod 2, (x, y) \in \{-1, 1\}$$

requires the introduction of additional auxiliary variables.

Free fermionic formulation of the heterotic string

The heterotic string is a hybrid construction that combines the 10-dimensional superstring with the 26-dimensional bosonic string.

In the free fermionic formulation of the heterotic string all world-sheet bosonic coordinates are fermionized (except the ones associated with 4D space-time). World-sheet supersymmetry is preserved as it is non-linearly realized among left moving fermions. In the standard notation the fermionic coordinates in the light-cone gauge are:

$$\begin{array}{lc|c|c} \text{Left:} & \psi^{\mu}, \chi^{1,\ldots,6}, & y^{1,\ldots,6}, \omega^{1,\ldots,6} & \\ \text{Right:} & & \bar{y}^{1,\ldots,6}, \bar{\omega}^{1,\ldots,6}, & \bar{\eta}^{1,2,3}, \bar{\psi}^{1,\ldots,5}, \quad \bar{\phi}^{1,\ldots,8} \end{array}$$

In this framework a model is defined by a set of basis vectors which encode the parallel transport properties of the fermionic fields along the non-contractible loops of the world-sheet torus, and a set of phases associated with generalised GSO projections (GGSO).

The string problem

We focus on a class of heterotic string models defined in the Free Fermionic Formulation using the basis $b = \{\beta_1, \ldots, \beta_{12}\}$, where

$$\begin{aligned}
\beta_1 = \mathbb{1} &= \{\psi^\mu, x^{1,\ldots,6}, y^{1,\ldots,6}, \omega^{1,\ldots,6}; \\
&\qquad \bar{y}^{1,\ldots,6}, \bar{\omega}^{1,\ldots,6}, \bar{\psi}^{1,\ldots,5}, \bar{\eta}^{1,2,3}, \bar{\phi}^{1,\ldots,4}, \bar{\phi}^{5,\ldots,8}\}\,, \\
\beta_2 = S &= \{\psi^\mu, x^{1,\ldots,6}\}\,, \\
\beta_{2+i} = e_i &= \{y^i\omega^i; \bar{y}^i, \bar{\omega}^i\}\,, i = 1, \ldots, 6\,, \\
\beta_9 = b_1 &= \{x^{34}, x^{56}, y^{3,4}, y^{5,6}; \bar{y}^{3,4}, \bar{y}^{5,6}, \bar{\psi}^{1,\ldots,5}, \bar{\eta}^1\}\,, \\
\beta_{10} = b_2 &= \{x^{12}, x^{56}, y^{1,2}, y^{5,6}; \bar{y}^{1,2}, \bar{y}^{5,6}, \bar{\psi}^{1,\ldots,5}, \bar{\eta}^2\}\,, \\
\beta_{11} = z_1 &= \{\bar{\phi}^{1,2,3,4}\}\,, \\
\beta_{12} = z_2 &= \{\bar{\phi}^{5,6,7,8}\}\,,
\end{aligned}$$

and a set of phases $c\left[\begin{smallmatrix}\beta_1\\ \beta_1\end{smallmatrix}\right] = \pm 1, c\left[\begin{smallmatrix}\beta_i\\ \beta_j\end{smallmatrix}\right] = \pm 1, i > j = 1, \ldots, 6$. The basis vectors β_i describe the parallel transportation properties of the fermionic coordinates along the world-sheet torus while the phases link to generalised GSO projections (GGSO).

A class of $SO(10)$ heterotic string compactifications

For $c\left[\begin{smallmatrix} S \\ e_i \end{smallmatrix}\right] = c\left[\begin{smallmatrix} S \\ z_a \end{smallmatrix}\right] = -1, i = 1, \ldots, 6, a = 1, 2$ and generic choice of the remaining GGSO phases, the above basis describes $\mathcal{N} = 1$ supersymmetric models. The gauge symmetry is

$$SO(10) \times U(1)^3 \times SO(8)^2$$

For the purpose of this analysis we consider $SO(10)$ as the observable gauge group. The massless string spectrum consists of states transforming in the $SO(10)$ vectorial representation **10** and states transforming in the $SO(10)$ spinorial representations $\mathbf{16}/\overline{\mathbf{16}}$.

The details of each model, including the number of vectorial $n_{\mathbf{10}}$ and the numbers of spinorial/antispinorial $n_{\mathbf{16}}/n_{\overline{\mathbf{16}}}$ representations are determined by the GGSO phases $c\left[\begin{smallmatrix} \beta_i \\ \beta_j \end{smallmatrix}\right]$.

By simple counting, this class comprises $2^{12(12-1)/2+1-8} = 2^{59} \sim 10^{17.8}$ distinct models.

Phenomenological characteristics and constraints

$SO(10)$ spinorials $(\mathbf{16}/\overline{\mathbf{16}})$ arise from the sectors $\mathcal{S}^I_{\vec{P}^I_s} = S + b_I + \vec{P}^I_s \cdot \vec{E}$, $I = 1, 2, 3$ where $P^1_s = (0, 0, p^1_s, q^1_s, r^1_s, s^1_s)$, $P^2_s = (p^2_s, q^2_s, 0, 0, r^2_s, s^2_s)$, $P^3_s = (p^3_s, q^3_s, r^3_s, s^3_s, 0, 0)$ and $\vec{E} = (e_1, e_2, e_3, e_4, e_5, e_6)$. Here, $b^3 = b^1 + b^2 + x$ with $x = \mathbb{1} + S + \sum_{i=1}^{6} e_i + \sum_{a=1}^{2} z_a$.

Similarly, $SO(10)$ vectorials $(\mathbf{10})$ come from the sectors $\mathcal{V}^I_{\vec{P}^I_v} = S + b_I + x + \vec{P}^I_v \cdot \vec{E}$, $I = 1, 2, 3$ where $P^1_v = (0, 0, p^1_v, q^1_v, r^1_v, s^1_v)$, $P^2_s = (p^2_v, q^2_v, 0, 0, r^2_v, s^2_v)$, $P^3_v = (p^3_v, q^3_v, r^3_v, s^3_v, 0, 0)$.

Phenomenological characteristics and constraints

Spinorial/vectorial representation projectors can be recast in the form

$$\boxed{\Delta^I U_s^I = Y_s^I \mod 2\,, \Delta^I U_v^I = Y_v^I \mod 2\,,\ I = 1,2,3\,,}$$

where, using $c\begin{bmatrix} b_i \\ b_j \end{bmatrix} = e^{i\pi(b_i|b_j)}$,

$$\Delta^1 = \begin{pmatrix} (e_1|e_3) & (e_1|e_4) & (e_1|e_5) & (e_1|e_6) \\ (e_2|e_3) & (e_2|e_4) & (e_2|e_5) & (e_2|e_6) \\ (z_1|e_3) & (z_1|e_4) & (z_1|e_5) & (z_1|e_6) \\ (z_2|e_3) & (z_2|e_4) & (z_2|e_5) & (z_2|e_6) \end{pmatrix}, Y_v^1 = \begin{pmatrix} (e_1|b_1+x) \\ (e_2|b_1+x) \\ (z_1|b_1+x) \\ (z_2|b_1+x) \end{pmatrix}, Y_s^1 = \begin{pmatrix} (e_1|b_1) \\ (e_2|b_1) \\ (z_1|b_1) \\ (z_2|b_1) \end{pmatrix},$$

where

$$U_s^{1\,T} = \begin{pmatrix} p_s^1 & q_s^1 & r_s^1 & s_s^1 \end{pmatrix}, V_s^{1\,T} = \begin{pmatrix} p_v^1 & q_v^1 & r_v^1 & s_v^1 \end{pmatrix}$$

and similarly for $\Delta_2, \Delta_3, Y_s^2, Y_s^3, U_s^2, U_s^3$, with $p_s^I, q_s^I, r_s^I, s_s^I, p_v^I, q_v^I, r_v^I, s_v^I = 0, 1, I = 1, 2, 3$.

Phenomenological characteristics and constraints

For a given solution U_s^I spinorial chiralities, $X^{(I)}_{pqrs} = \mathbf{exp}(i\pi\chi^{(I)}_{pqrs})$, are computed using

$$\begin{aligned}\chi^{(1)}_{pqrs} = &(1-r)(e_5|b_1) + (1-s)(e_6|b_1) + p(e_3|b_2) + q(e_4|b_2) \\ &+ r(e_5|b_2) + s(e_6|b_2) + p(1-r)(e_3|e_5) + p(1-s)(e_3|e_6) \\ &+ q(1-r)(e_4|e_5) + q(1-s)(e_4|e_6) + (r+s)(e_5|e_6)\,,\end{aligned}$$

and similarly for $X^{(2)}_{pqrs}, X^{(3)}_{pqrs}$.

Conventions and constraints

For a given set of spin structure coefficients $c\begin{bmatrix}\beta_i\\ \beta_j\end{bmatrix}$ the solutions $U_s^I, U_v^I, I = 1,2,3$, that is $\Xi_s^I = \{p_s^I, q_s^I, r_s^I, s_s^I\}$, $\Xi_v^I = \{p_v^I, q_v^I, r_v^I\}$, with $p_s^I, p_v^I, s_v^I \in \{0,1\}$, determine the number of surviving spinorials/ vectorials, that is the phenomenology of the model. We impose

$$\boxed{N_F \;=\; \sum_{I=1}^{3}\left(\sum_{p,q,r,s\in\Xi_s^I} X^{(I)}_{pqrs}\right) \;=\; 3\,,(\text{3 fermion generations})}$$

and also

$$\boxed{N_H \;=\; \sum_{I=1}^{3}\left(\sum_{p,q,r,s\in\Xi_v^I} 1\right) \geq 1\,,(\text{at least one MSSM Higgs multiplet})}$$

and also the existence of a coupling of the form

$$\boxed{\boxed{\mathbf{16}\times\mathbf{16}\times\mathbf{10},(\text{top quark mass Yukawa coupling})}}$$

Quantum annealer implementation

All (solvable) constraints and conventions taken into account we are left with 28 independent GGSO coefficients, that is $2^{28} \sim 10^8$ models.

The reduced problem Hamiltonian can be recast in the form

$$H = \sum_{i=1}^{4} \left(\Delta^3_{ij} U^3_{s,j} - Y^3_{s,i} - 2K_i \right)^2 + \sum_{i=1}^{4} (\Delta^1_{ij} U^1_{v,j} - Y^1_{v,i} - 2K_{4+i})^2 + \sum_{i=1}^{4} (\Delta^2_{ij} U^2_{v,j} - Y^2_{v,j} - 2K_{8+i})^2 + \left(\chi^{(3)}_{pqrs} - 2K_{13} \right)^2 ,$$

where $K_{i=1,\ldots,13}$ are auxiliary variables required for the **mod** 2 reduction.

In order to perform our analysis the system was implemented on D-Wave's *Advantage_system4.1* architecture: this annealer contains 5627 qubits, connected in a *Pegasus* structure, but only has a total of 40279 couplings between them.

Quantum annealer implementation

Classical post-processing is required in order ro satisfy some of the constraints as the annealer is not good at counting solutions.

To compare the different methods we first perform a comprehensive scan of this system: this took about 48 hours on a DELL PowerEdge R630 workstation with 32 GB of memory which resulted in a total number of 1024 acceptable models.

We have also analysed the problem using other standard methods including: Random scan, Simulated annealing, Genetic algorithm.

Results

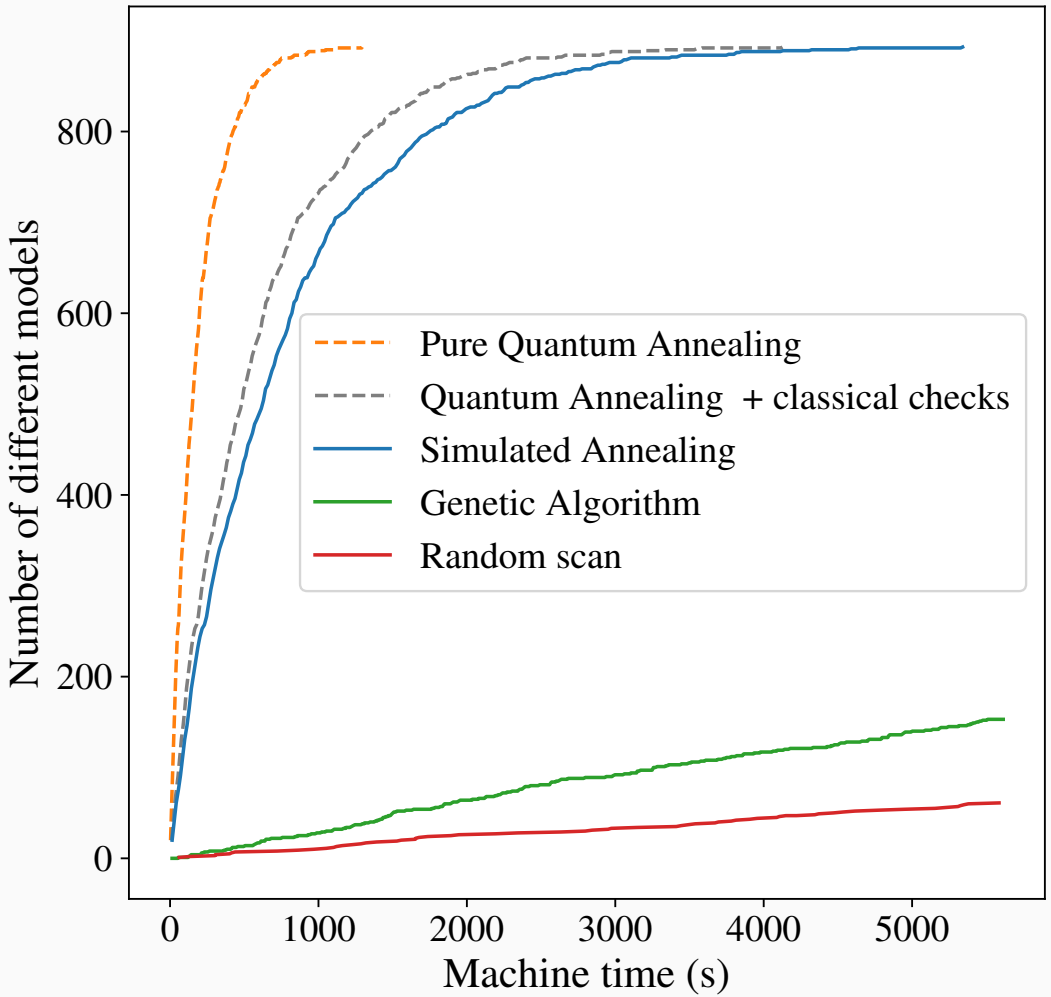

Figure 2: Comparison of the machine-time efficiency of various techniques for finding viable models. The methods analysed are: random scans, genetic algorithms, simulated annealing and quantum annealing.

Results

The initial model discovery rate (i.e., within the first 1000s) is one model in 0.66 seconds for simulated annealing, compared to one models in 33 seconds for the genetic algorithm and one in 100 seconds for the random scan. Using quantum annealing, the rate increases to one model in 0.50 seconds when model checks are performed classically.

Conclusions

We have employed quantum annealing (QA) to construct string models, focusing on their efficiency and effectiveness in the model discovery process. By comparing quantum annealing with other established methods such as simulated annealing, random scans, and genetic algorithms, we have gained valuable insights into the possible advantages of using quantum annealers for this purpose.

It seems that quantum annealers outperform other methods when the search space consists of relatively dense regions of SM-like models (in this study one model in 10^5).

Therefore, it would be interesting in future investigations to compare QA methods in more difficult problem domains in order to provide a comprehensive assessment of their respective strengths and weaknesses.